University of Baghdad
College of Engineering
JE
JOURNAL OF ENGINEERING

Journal of Engineering
journal homepage: www.jcoeng.edu.iq
Volume 30 Number 9 September 2024

Ultimate Capacity and Load Transfer Mechanism of Ground Anchors in Granular Soils: State-of-the-Art

Nadher H. Al-Baghdadi [1,*], **Balqees A. Ahmed** [2]

[1] Department of Civil Engineering, Faculty of Engineering, University of Kufa, Al-Najaf, Iraq
[2] Department Civil Engineering, College of Engineering, University of Baghdad, Baghdad, Iraq

ABSTRACT

The grouted ground anchor is the most used geotechnical element to transfer the tension load from the superstructure or the soil mass in front of the potential failure surface (active zone) to a deeper, efficient soil layer for its reliability and feasibility. It was originally constructed by inserting the tendon, usually a steel strand, into an already drilled borehole filled with cement grout. It was successfully used in the Cheurfas dam in Algeria in (1934). According to the load transfer mechanism, there are two types of ground anchors: tension-type and compression-type. The names of these two types of anchors refer to the developed stresses in the grouted body. The present work presents a literature survey about the load transfer mechanism for both types of anchors: tension and compression embedded in granular soil. Many factors affecting the load transfer mechanism have been reviewed. The main factor affecting the load transfer mechanism is the confining pressure of the borehole. The recently developed methods of estimating the ultimate pullout capacity of the anchor have been reviewed and discussed.

Keywords: Ground anchor, Load transfer mechanism, Ultimate pullout capacity.

1. INTRODUCTION

Grouted ground anchor, sometimes called tie-back or tie-down, is a construction element used to transmit the tensile force to the bearing stratum of the ground (rock or soil). The grouted ground anchor consists mainly of a tendon, usually made of a steel strand or a steel bar. A fiber-reinforced polymer (FRP), aramid fiber-reinforced polymer (AFRP), or carbon fiber-reinforced polymer (CFRP) tendon is used in grouted ground anchors to improve corrosion resistance **(Ortigao, 1996; Zhang et al., 2001; Elias, 2019)**. The tendon is inserted in a grouted borehole. The direction of the borehole could be vertical, horizontal, or inclined. The resisting force is generated by stressing the tendon to a certain stress level according to the design. **Fig. 1** shows the components of the grouted ground anchor according to **(BS 8081, 1989)**.

*Corresponding author
Peer review under the responsibility of University of Baghdad.
https://doi.org/10.31026/j.eng.2024.09.08

Article received: 27/10/2023
Article revised: 03/01/2024
Article accepted: 18/01/2024
Article published: 01/09/2024

According to the load transfer mechanism, the grouted ground anchors can be classified into tension and compression. The tension anchor depends on the tension stresses developed in the grouted body to transfer the load from the tendon to the ground. In contrast, the compression anchor develops compression stresses in the grouted body to transfer the load. The tension-type anchor is shown in **Fig. 1**, while the compression-type is shown in **Fig. 2**.

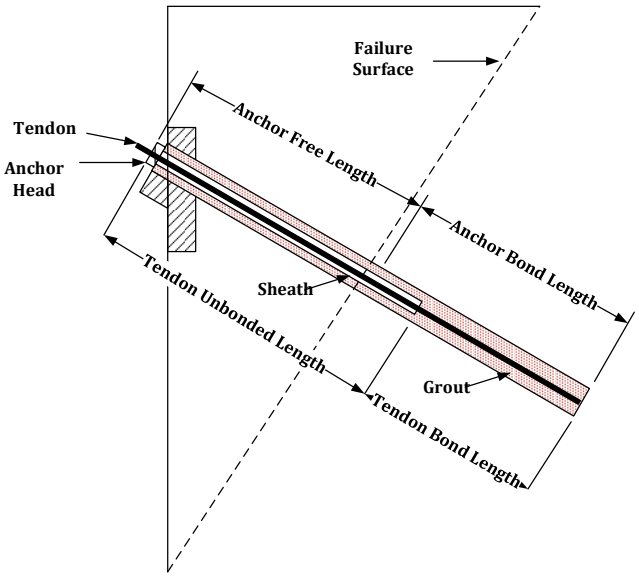

Figure 1. Tension-type ground anchor and parts **(BS 8081, 1989)**.

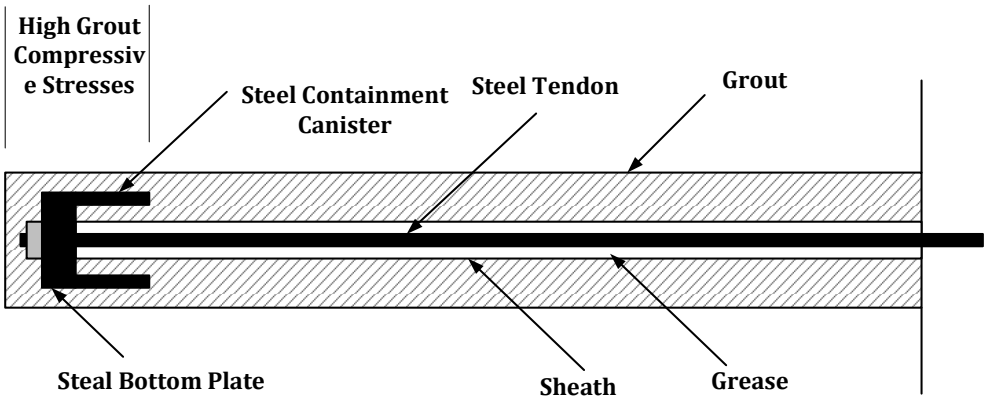

Figure 2. Compression-type ground anchor.

In the case of tension-type anchors, the load is transferred from the tendon to the grout along the bond length zone through the bond between the tendon and the grout, and then the load is transferred to the surrounding ground along a specified length of the anchor. In the compression-type case, the load is transferred from the tendon to the grout through the end-plate, which is located at the distal end of the bond length, as shown in **Fig. 2**, and then the load is transferred from the grouted body to the surrounding ground. Both mentioned anchor types depend on the assumption that there is no friction between the tendon and the encapsulation pipe along the free length in the case of the tension type or along the anchor length in the case of the compression type, so no load is transferred through this friction along the free length. The instruments field and physical model tests

are essential in understanding the load transfer mechanism through the valuable data provided by the strain gauges **(Popa et al., 2016)**.
This work presents the recent contributions in load transfer mechanism and the ultimate pullout capacity estimation methods for both types of anchors embedded in granular soils. The enhancements of the anchor components, which affect the load transfer mechanism and then the load ultimate pullout capacity, have been reviewed. Discussions on some findings and comparisons between methods and conclusions are also presented.

2. LOAD TRANSFER THROUGH TENDON

According to the recommendation of the Post Tension Institute **(PTI, 2014)**, tendon failure could be avoided by limiting the anchor design load and testing load by (60% and 80%) of the minimum specified strength of the steel tendon, respectively.
The applied load is transferred to the grout through the tendon along the bond length with some losses due to friction with the plastic sheath along the free length. The friction losses are estimated by comparing the "Apparent Free Length" with its minimum limit.
The apparent free length represents the theoretical tendon length calculated according to the measured elastic movement of the anchor head. The measured elastic movement is affected by the friction between the tendon and the plastic sheath during primary loading cycles (before debonding between the tendon and the grout occurs) and by the friction between the tendon and the grout after debonding occurs. Eq. 1 is used to calculate the apparent free tendon length based on Hook's law **(PTI, 2014)**.

$$L_a = \frac{A\ E\ \delta_e}{P} \tag{1}$$

where:
A) is the cross-section area of the tendon, (E) is the modulus of elasticity of the tendon, (δ_e) is the measured elastic displacement of the anchor head, (P) is the applied load.
The minimum limit of the apparent free length is equal to the jack height added to (80%) of the calculated free length **(PTI, 2014)**. When the apparent free tendon length is less than its minimum limit, it indicates that a portion of the applied load is transferred along the free length through friction **(FHWA, 1999; PTI, 2014)**. Load transferring through the free-length part is undesirable because the free-length part is located at the active wedge in the case of retaining structures, and it could transfer the load to the structure itself in the rest of the cases.
(Ostermayer and Scheele, 1977) presented a stress distribution of the tendon along the bond length of the anchor embedded in dense sand, as shown in **Fig. 3**. The stress values were calculated from the measured strains obtained from electrical strain gauges attached to the tendon at certain locations. Stress values decrease from the proximal end until they vanish toward the distal end due to progressive debonding between the tendon and the grout.
All the measured stress distribution matches the shape of the stress distribution presented in **Fig. 3.** The stress distribution along the anchor bond length in different types of soils are reported previously. **(Evangelista and Sapio, 1978; Chalmovský and Miča, 2018)** reported and analyzed full-scale anchor tests embedded in a stiff clay formation. **(Weerasinghe and Littlejohn, 1997)** measured the developed stress along the tendon in the bond length part for full-scale anchors embedded in a weak mudstone.

(Ruggeri et al. 2020) reported the developed stresses along the threaded bar tendon of a full-scale anchor field test embedded in non-homogenous ground. **(Sousa et al., 2021)** reported the stress distribution along the tendon for a full-scale anchor constructed in sand. It can be concluded that the soil type where the anchor bond length is embedded does not affect the shape of the stress distribution, while these stresses value depends on many factors, such as tendon materials modulus of elasticity, tendon-grout bond stress, grout strength, and the applied load reached to the bond length proximal end.

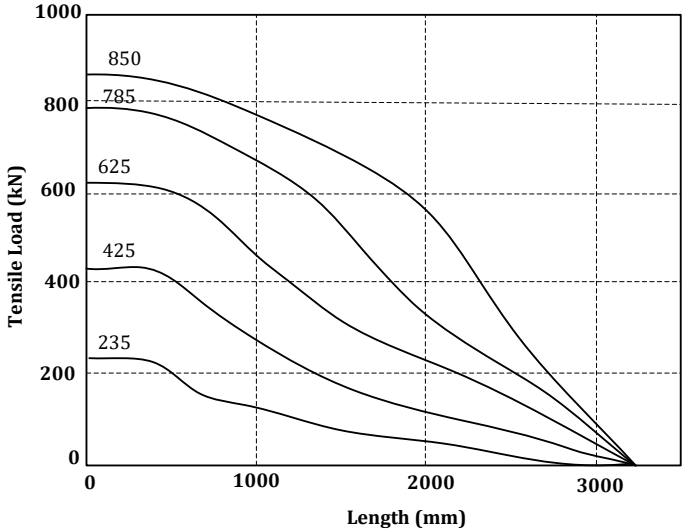

Figure 3. Load distribution along the tendon within the bond length **(Ostermayer and Scheele, 1977)**.

3. LOAD TRANSFER THROUGH TENDON GROUT INTERFACE

The applied load is transferred from the tendon to the surrounding grout by developing shear stresses within the anchor bonded length of the tension-type anchors. However, there is no tendon grout interface in compression-type anchors. The cracks in the grout will be developed when the principal tensile stresses exceed the maximum tensile strength **(Hanna, 1982)**. **Fig. 4** shows a schematic diagram of cracks development within the grouted body around the tendon in the bond length zone. The bond strength between the grout and the steel tendon contains three components (**Littlejohn and Bruce, 1975)**, as follows:

1) Adhesion contains the chemical bond **(Hanna, 1982)** and physical interlock due to the tendon surface toughness on the microscopic scale.

2) Friction, which depends mainly on the surface characteristics of the tendon and the magnitude of the slippage that occurred. The confining pressure, dilatancy, and wedge action significantly contribute to this component.

3) Mechanical interlock occurs due to tendon ribs, twists, and/or strand nodes.

Nodes are made with a single strand (local nodes) or by wrapping the parallel strands. **Fig. 5** shows the types of nodes with strands. According to **(Barley, 1978),** using the general nodes enhances the bond stress between the tendon and the grout by more than (100%) when using a bond length up to 1.5m, while the enhancement reaches (40%) when using a bond length between 1.4 to 2.2m. Through experimental field tests, **(Adams and Littlejohn, 1997)** concluded that using general nodding by wrapping the parallel strand increases the tendon-grout average bond strength by (164%) while using local nodes concentrated in the same location enhances the bond capacity by (70%).

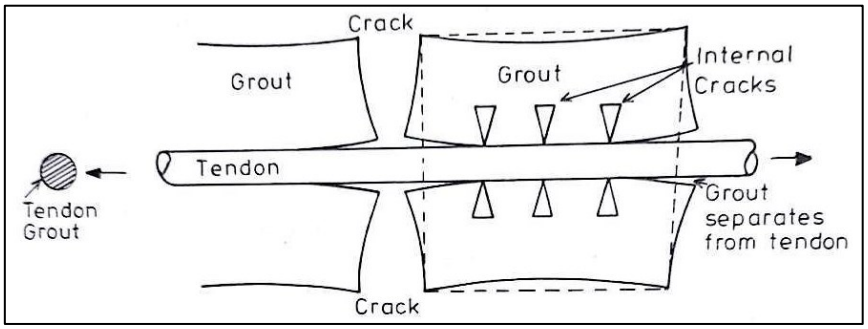

Figure 4. Schematic diagram of crack development within the grouted body around the tendon in the bond length **(Hanna, 1982)**.

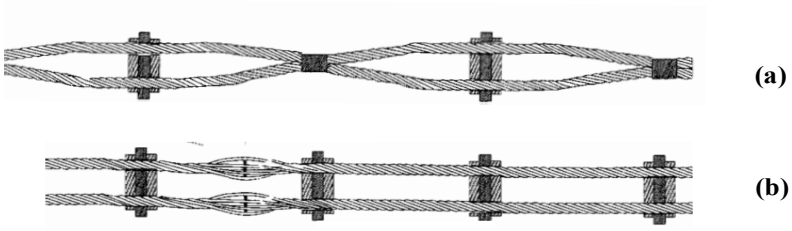

Figure 5. Types of nodes with strands, (a) general nodes, and (b) local nodes **(Adams and Littlejohn, 1997)**.

The bond resistance depends on the adhesion in the first place, where there is no relative displacement between the tendon and grout. Due to the relative displacement initiation, the adhesion component vanishes, and the other components are raised. This operation starts from the proximal end of the bond length and moves toward the distal end progressively. **Fig. 6** shows the relation between tendon-grout bond strength and relative displacement.

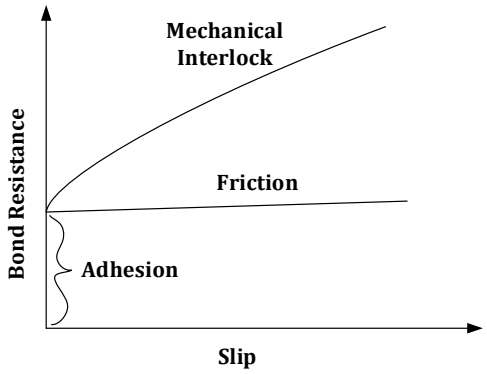

Figure 6. Components of the bond between tendon and grout **(Littlejohn, 1975)**.

3.1 Effect of Grout Strength

Based on the results of 500 pullout tests of strands embedded in concrete, **(Stocker and Sozen, 1969)** concluded that the strand concrete bond increases by about (10%) per each (7MPa) of increasing concrete strength for concrete strength ranging between (16.6-52.4MPa). The bond stress between the tendon (deformed bar and strand) and the grout is proportional to the square root of the unconfined compressive strength of the grout **(Brown, 1970; Laldji and Young, 1988)**. However, **(Littlejohn, 1979)** suggested

the minimum compressive strength of the grout is 40MPa to provide enough bond and shear strength.

3.2 Effect of Confining Pressure

Many researchers have studied the effect of confining pressure on the grout-tendon bond strength; the main findings are listed below:

(Lo, 1979) conducted a series of pullout tests of a (50mm) diameter steel bar placed in grout. The grout is confined with steel tubes with different inner diameters ranging between (100mm to 155mm). The pullout capacity increased with increased grout diameter (confining tube diameter). **Fig. 7** shows the relation between the pullout capacity and confining diameter.

Another series of tests was conducted by the same researcher using different wall thickness confining steel tubes and rubber hoses with different degrees of stiffness to model different types of weak and dense sands according to their modulus of elasticity. These tests have been classified into three categories of confinements: non confined, partially confined, and fully confined. The bond capacity increased with the elastic modulus of the confining tubes, representing the confinement condition of the ground. The researcher has discovered different shapes of failure according to confinement states. In the case of no confinement and partial confinement states, the failure occurred by bursting the grouted body. While in the fully confined state, the failure occurred by shear along the contact surface between the bar and the grout.

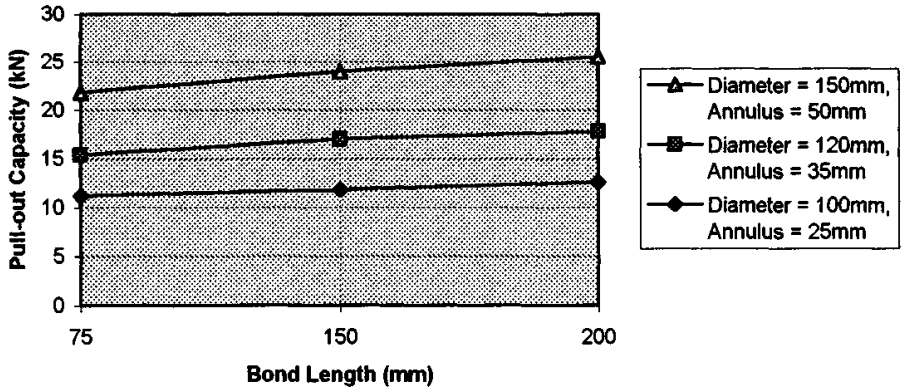

Figure 7. Relation between the grout diameter and pullout capacity **(Lo, 1979)**.

(Laldji and Young, 1988) investigated the bond stress between the tendon (strand) and the grout (cement-based grout) through laboratory pullout tests of a strand embedded into cement grout cubes subjected to different confining pressures. They concluded that the bond stress increases by 1MPa for every 3MPa increment of confining pressure until the bond stress reaches (0.3 f_{cu}) of grout; beyond this value, the bond stress is increased with the confining pressure increment.

(Kaiser et al., 1992) have conducted experimental pullout tests of smooth, polished, rounded section bars embedded in grout and cast in a thick-walled granite cylinder. Lateral confining pressure was applied to the rock cylinder using a Hoek triaxial cell (HTC). Before each test, a small torque was applied to the rod to break the cohesive bond between the rod and the grout to make the results related only to the friction component. The test results generally show a linear increase in the bond stress with lateral confining applied stress change (Δp_3), as shown in **Fig. 8**.

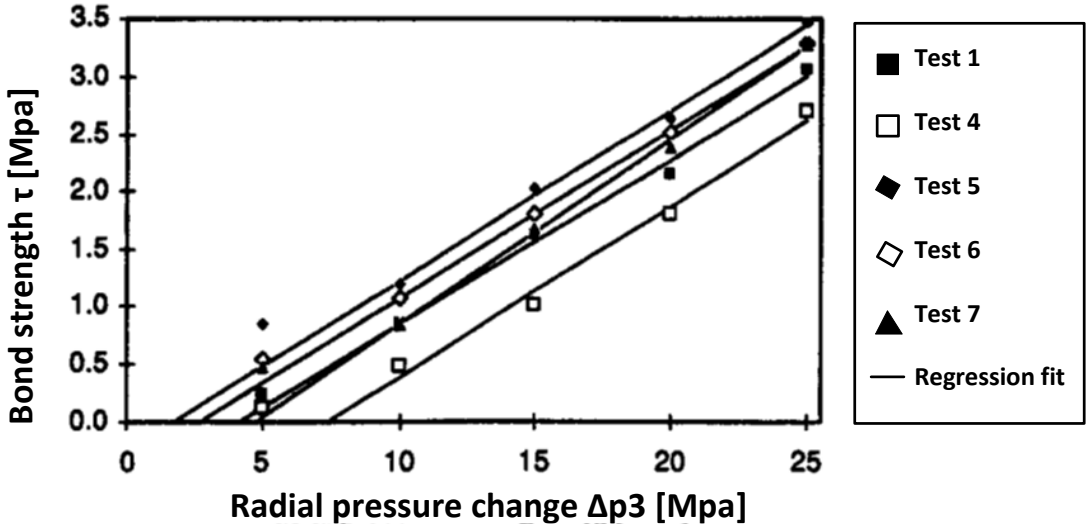

Figure 8. Relation between the confining pressure variation and the bond stress's frictional component **(Kaiser et al., 1992)**.

(Hyett et al., 1992) conducted laboratory and field pullout tests to investigate the effect of radial confinement on the bond capacity of grouted bolts. A prestress strand 15.9mm diameter was embedded in the grout. In the laboratory tests, the grout is confined with different material tubes to simulate different radial stiffnesses, while in the field tests, different types of rocks with different moduli of elasticity to provide different radial stiffnesses were bored and grouted. The researchers concluded that as the radial stiffness increased, the failure mechanism of the grouted body transformed from radial cracking and lateral displacement to the shear and pullout of the grout cylinder surrounding the strand. **(Hyett et al., 1995)** performed a series of pullout tests of grouted strand cable. The grout was subjected to confining pressure by a modified Hoek triaxial cell. The bond strength between the strand and the grout increases with the increase of confining pressure**. Fig. 9** shows the relation between the confining pressure and the bond strength. **(Jarred and Haberfield, 1997)** have studied the effect of confining pressure on the bond strength between the tendon and the grout by studying the radial stiffness of the borehole. They suggested Eq. 2, which presents the radial stiffness of the borehole:

$$K = \frac{\Delta\sigma}{\Delta r} = \frac{E_m}{1+v_m} \times \frac{1}{r} \quad (2)$$

where: (E_m), and (v_m) are the modulus of elasticity and Poisson's ratio of the ground
r is the radius of the borehole.
Their experimental work related the maximum shear and bond strength between the tendon and the grout with confining stiffness, as shown in **Fig. 10**.
(Chamberlain, 1993) (as cited in Jarred and Haberfield, 1997), has proved theoretically that the relatively high confining stiffness (> 80MPa/mm) would increase the bond strength between the tendon and the grout. **(Shokri et al., 2023)** conducted a series of pullout tests for a 16mm diameter reinforcement bar embedded by 50mm into grout molded with steel tubes with two different inner diameters 23mm and 50mm. The results showed that the bond has increased by 45% in the case of a larger confining diameter.

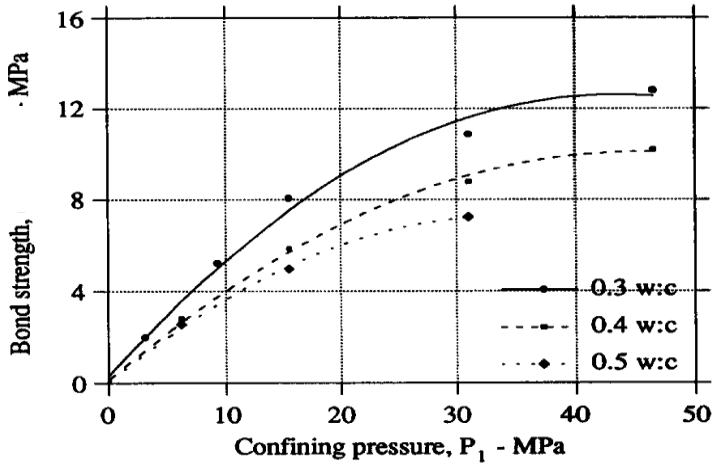

Figure 9. The effect of confining pressure on the bond stress with the effect of grout (w/c) ratio **(Hyett et al., 1995)**.

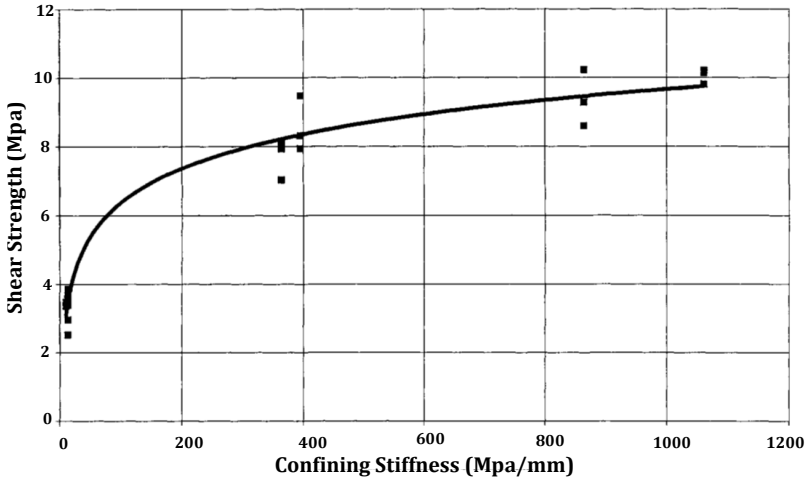

Figure 10. Confining stiffness vs shear strength **(Jarred and Haberfield, 1997)**.

One of the most effective methods to increase the confining pressure is using expansive cement, which forces the grout to expand against the surrounding ground. Expansive cement was also suggested to reduce shrinkage due to grout drying **(Jarred and Haberfield, 1997; Benmokrane et al., 1995)**.

3.3 Bond Stress Distribution

Progressive debonding occurs from the proximal end. Due to load increment, the location of the peak bond stress moves towards the distal end, while the residual bond strength remains effective with nearly uniform distribution along the length where the peak stress has moved from (**Littlejohn and Bruce, 1975; Ostermayer Scheele, 1977; Barley, 1988**). This behavior was reported by **(Gilkey et al., 1940) (As cited in Littlejohn and Bruce, 1977)** by studying plain embedded steel bars in concrete. **Figs. 11 and 12** show the progressive debonding between the tendon and the grout and the bond stress distribution along the bond length at successive stages of loading. Due to the different

elastic moduli between the tendon and the grout materials, the bond stress distribution is not uniform along the bond length. **(Barley, 1988; Barely and Windsor, 2000)**.

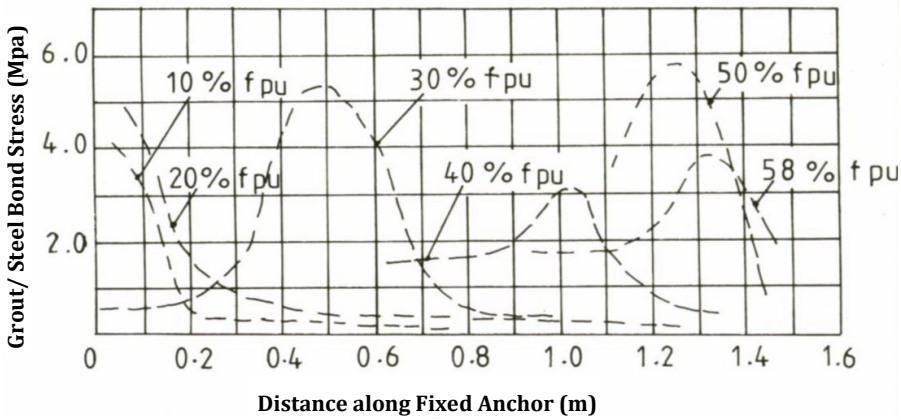

Figure 11. Bond stress distribution between the tendon and the grout during loading stages (load as a percent of f_{pu}) **(Gilkey et al., 1940)**.

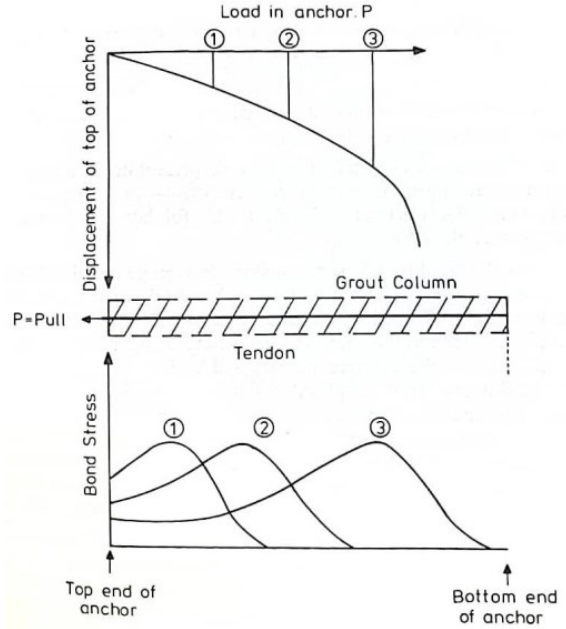

Figure 12. Progressive deboning between the tendon and the grout along tendon bond length during loading **(Hanna, 1982)**.

Both at low-stress levels and during failure, the fixed anchor length's stress distribution is not uniform. The elastic modulus and associated deformation of the anchor strands, cement grout, and surrounding ground are generally incompatible, which leads to this phenomenon (**Barley, 1988; Barely and Windsor, 2000**).
To overcome the full debonding between the tendon and the grout, **(Littlejohn et al., 1977)** suggested the minimum bond length to be equal to 3m.

4. LOAD TRANSFER THROUGH GROUTED BODY

The grouted body transfers the load from the tendon to the surrounding soil through shear and direct bearing in the confined state, in both anchors, tension, and compression

(Barley, 1997). In tension-type anchors, the grouted body is subjected to two stresses: tension stresses in the bond length part and compression stresses in the free length part of the grouted body **(Briaud et al., 1998)**. While in compression-type anchors, the grouted body is subjected only to compression stresses **(Barley, 1997)**.

The grouted body needs to satisfy a certain level of strength to resist these developed stresses. The unconfined compression strength **(ASTM C109/C 109M, 2002)** is used to specify the grout strength requirements of the hardened grout. The minimum unconfined compression strength of the grout is 21MPa according to **(FHWA, 1999)**, while **(Littlejohn, 1980)** was more conservative and suggests a 40MPa grout strength at 28 days of age. The most effective factor on the grout strength is the water-cement (w/c) ratio, commonly taken within different ranges according to different standards and researchers. However, the wider range of the (w/c) ratio is recommended by the German code **(DIN 4125, 1990)**, which ranges between (0.35-0.7). The (w/c) varied according to the soil type. Usually, the higher ratio is used for cohesionless soils to avoid the water reduction of grout due to the permeable environment of the soil.

The grout has a very low tensile strength compared with the compression strength. The tensile strength of the grout is about (0.133) of the Unconfined compressive strength **(Coulter and Martin, 2006)**, which is much less than the tension stresses developed in the bond length of the tension-type anchor. **(Klemenc and Logar, 2013)** conducted field tests with improved grout stiffness by reinforcing the total bond length. The reinforced anchor exhibited a (16%) increase in load-carrying capacity. **(Barley, 1997)** concluded that the unconfined compression strength provides neither information nor guidance on the actual strength of the grouted body. However, the grout strength is highly affected by the degree of confinement. The above conclusion has been made depending on the results of a series of unconfined compression tests compared with the results of confined bearing tests **(Barley, 1978 and 1996)**. **Fig. 13** shows a comparison between unconfined and confined compression strength for ordinary cement grout and proprietary grout, which is a special type of grout containing polymer and additives.

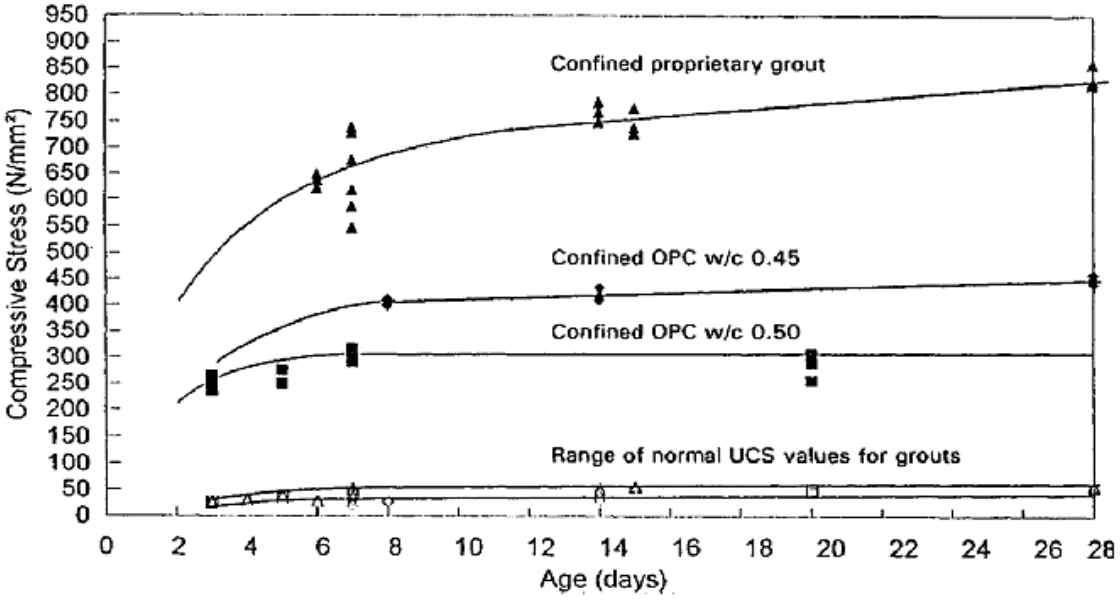

Figure 13. Comparison between the unconfined and confined compression strength of grout **(Barley, 1997)**.

5. LOAD TRANSFER THROUGH GROUT-GROUND INTERFACE

The load is transferred from the grouted body to the surrounding soil by the shear stresses between the grout and the ground **(Barley and Windsor, 2000)**. When the value of the bond stress reaches its ultimate value at one of the interfaces, tendon-grout or grout-soil, the other interface bond stress cannot be increased. This part of the anchor length has reached the ultimate capacity; the bond stress will decrease subsequently. When the applied load increased, the stress peak zone shifted towards the distal end of the bond length. The peak bond stress zone reaches the distal end before failure occurs **(Barley and Windsor, 2000)**. **Fig. 14** shows the bond stress distribution during the loading process along the bond length.

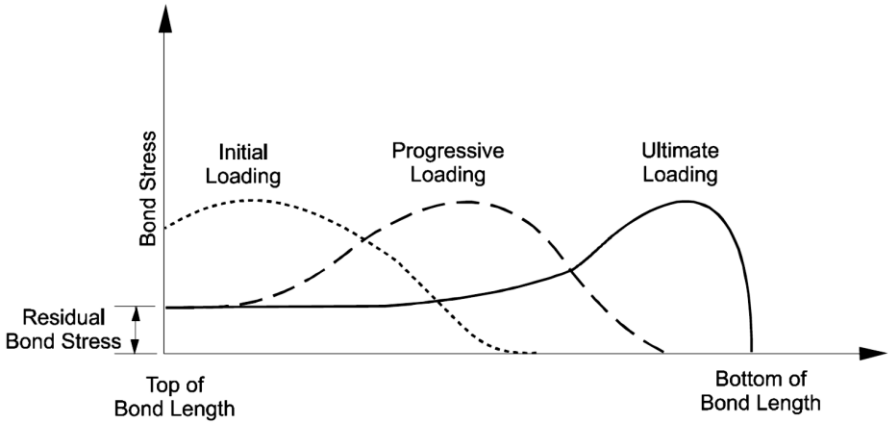

Figure 14 Bond stress distribution during the loading process along the bond length of tension-type anchor **(Barely and Windsor, 2000)**.

The bond strength between the grout and the soil mainly depends on the normal stress acting on the interface, which may exceed the stress developed due to overburden by (2-10) times. This phenomenon is called the locking-in effect, which increases with the increase of the relative density and uniformity coefficient. The locking-in effect is caused by the dilation of the dense sand subjected to shear, which increases the redial stress **(Ostermayer, 1975)**. The grout-ground bond stress depends on construction techniques and soil properties **(Awad-Allah, 2018)**. The construction techniques include borehole drilling and grouting methods, while the soil properties include the relative density, angle of internal friction, and grain size distribution **(Juran and Elias, 1991)**. The dense soil produces a several times higher value of grout-ground bond stress than the value produced in loose or medium-dense soils because of the interlocking effect caused by soil dilation **(Ostermayer, 1975; Wernick, 1977)**.

According to **(Ostermayer, 1975)**, for the same soil density, the ultimate stress increases with the increase of the coefficient of uniformity.

(Fujita et al., 1977) submitted a relationship between the SPT value of granular soils and the ultimate average grout-ground bond stress of the grout-ground interface. This relation has been extended by **(Bustamante and Doix, 1985) (as cited by Juran and Elias, 1991)** by introducing other researchers' data, as shown in **Fig. 15**.

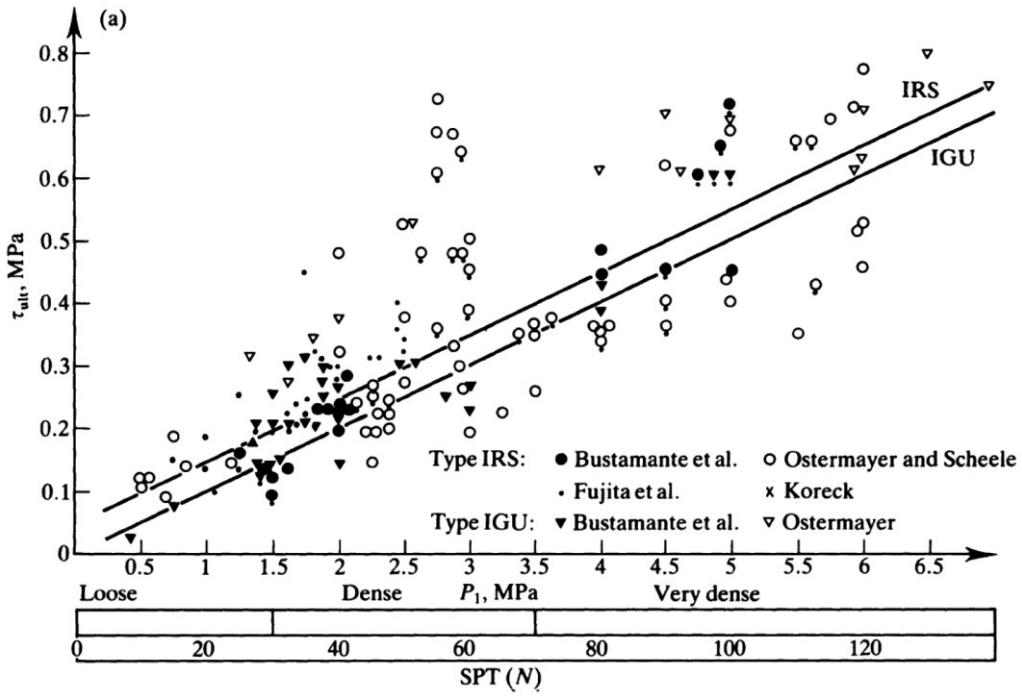

Figure 15. Relation between the mean SPT value for a single stratum of granular soil and maximum skin friction, where IGU is single-stage grouting, and IRS is a multiple-stage post-grouting **(Bustamante and Doix, 1985)**.

Through many field tests in granular soils, stated the following conclusions:
The value of grout-ground bond stress is decreased with the increase of the bond length and the diameter of the grouted body independently, as shown in **Fig. 16**; therefore, it is not feasible to increase the bond length to obtain a higher ultimate pullout capacity. From an economic point of view, the optimal bond length ranges between 6 and 7m, as shown in **Figs. 17 and 18**. However, when the diameter of the grouted body increases more than (100mm), there is no significant increase in the ultimate pullout capacity.

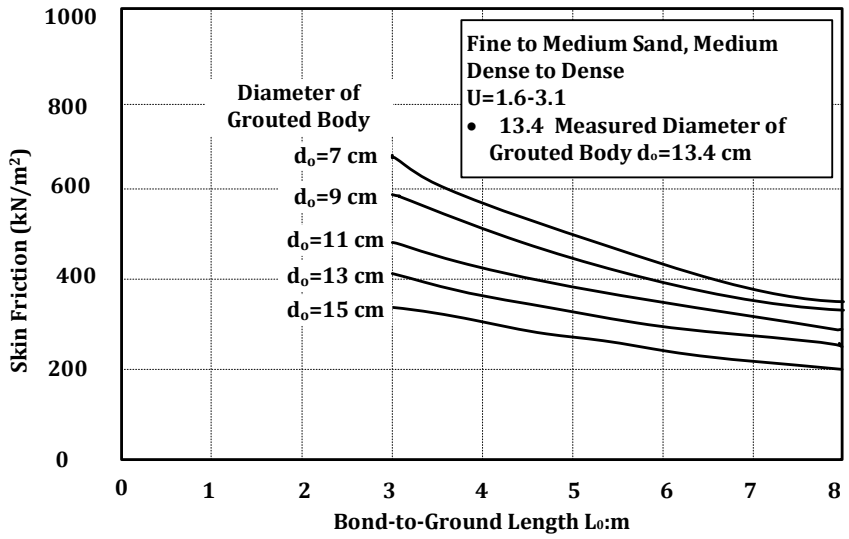

Figure 16. Influence of anchor diameter and bond length on the grout-ground bond stress **(Ostermayer, 1975)**.

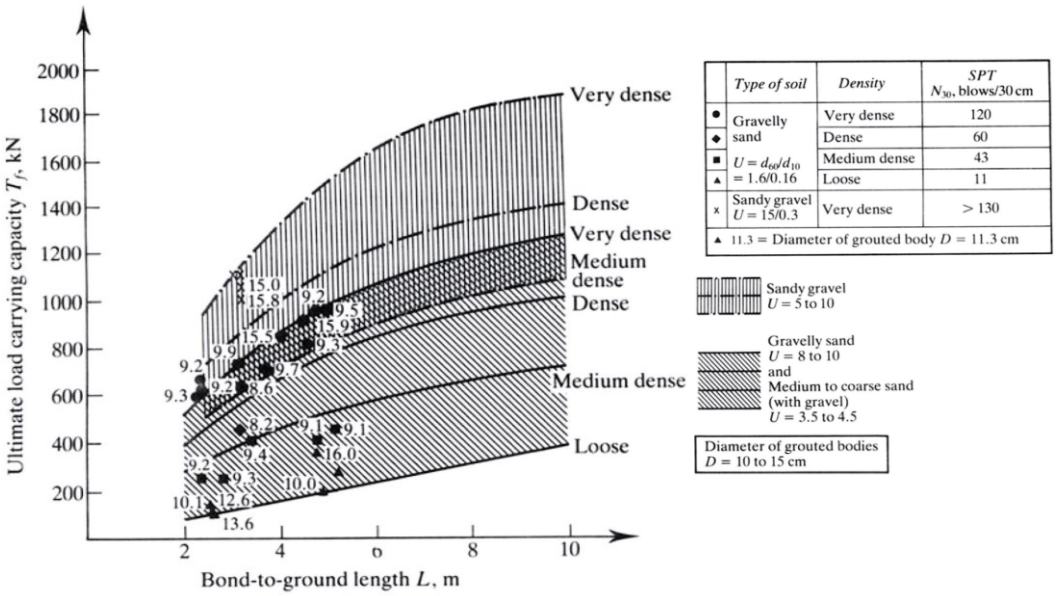

Figure 17. Influence of soil type and bond length on the ultimate pullout capacity **(Ostermayer, 1975)**.

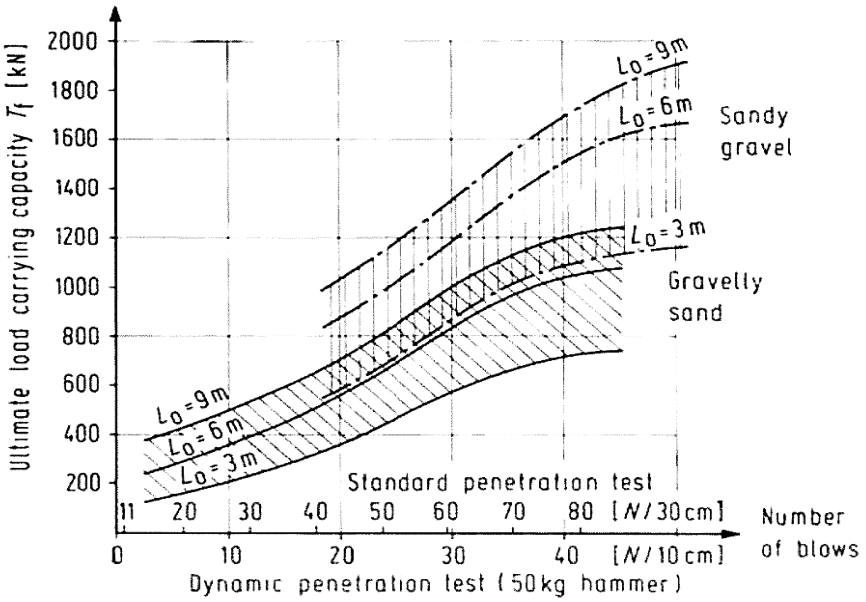

Figure 18. Ultimate anchor capacity vs. the spt number for three fixed anchor lengths of non-cohesive soils **(Ostermayer and Scheele, 1977)**

5.1 Distribution Of Grout- Ground Bond Stress

(Ostermayer and Scheele, 1977) have performed and reported a series of field tests of thirty tension-type grouted ground anchors embedded in a sandy gravel layer and gravely sand layer with variable densities from loose to very dense. The tested anchors were instrumented with strain gauges attached to the steel tendon (prestressed bar) to measure the developed strain along the tendon. The grout-ground bond stress between the grout and the ground is calculated according to the measured strain along the tendon,

assuming that it is the same strain along the grouted body if the developed strain does not exceed the cracking or the debonding values ($1*10^{-4}$) **(Briaud et al., 1998)**. However, the grout-ground bond stress of the tested anchors along the bond length is shown in **Fig. 19**. It is noticed that the grout-ground bond stress is not uniformly distributed as **(Ostermayer, 1975)** stated previously.Through field tests of instrumented ground anchors, the non-uniform distribution of grout-ground bond stress along the bond length was observed by **(Mastrantuono and Tomiolo, 1977; Sousa et al., 2021; Iten and Puzrin, 2010)**. The measurements were made by using strain gauges attached to the tendon, which cannot measure the strain developed inside the grouted body after debonding between the tendon and the grout had occurred, as mentioned previously.

The grout-ground bond stress along the entire length of the anchor has been reported by **(Kim, 2001)** through field tests of one-stage gravity grouted, compression, and tension-type anchors. The tested anchors were embedded in stratified soil. The bond length of the tension-type anchor was entirely embedded in weathered cohesionless strata. It is substantial to mention that the researcher used two types of strain gauges; the first type was attached to the tendon to measure the strains along it, and the other type of strain gauge was embedded into the grouted body to measure the developed strains along the entire length of the grouted body directly from the grout, regardless of the debonding between the tendon and the grout. **Figs. 20 and 21** show the measured grout-ground bond stress along the length of both tension and compression anchors, respectively. It is noticed that there is no effect of the soil stratification on the grout-ground bond stress magnitude or distribution, especially on the compression-type anchor. The non-uniform distribution of grout-ground bond stress along the bond length of the tension-type anchor is noticed, while the grout-ground bond stress magnitude is very small and distributed descendingly along the free-length part. In the case of the compression-type anchor, the grout-ground bond stress is concentrated at the lower one-third of the anchor length and vanishes toward the anchor head. **(Al-Baghdadi and Ahmed, 2022)** presented the grout-ground bond stress along the total anchor length through strain measurement of a full-scale field test of an instrumented ground anchor embedded in sandy soil. The strain gauges were installed on the corrugated protection sheath to avoid unrealistic measurements after tendon-grout debonding.

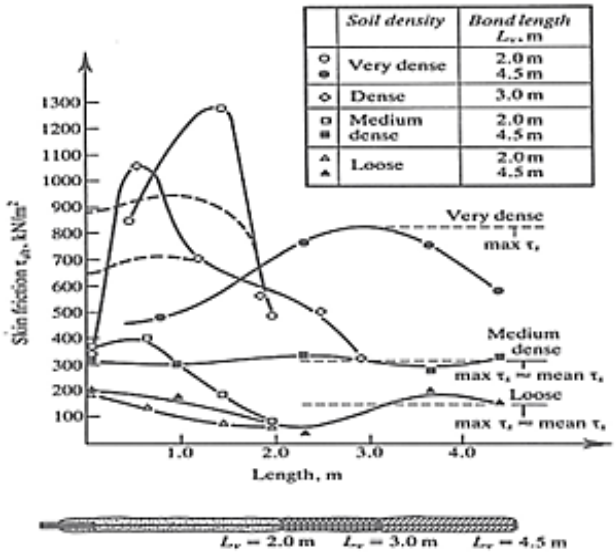

Figure 19. Distribution of grout-ground bond stress along the bond length **(Ostermayer and Scheele, 1977)**.

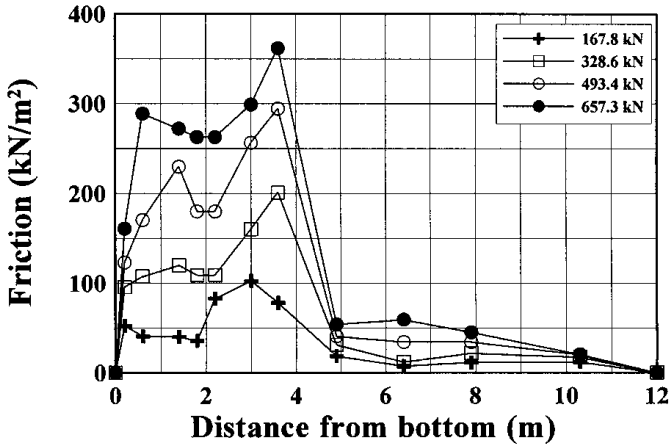

Figure 20. Grout-ground bond stress along the entire length of the ground anchor for tension-type anchor **(Kim, 2001)**.

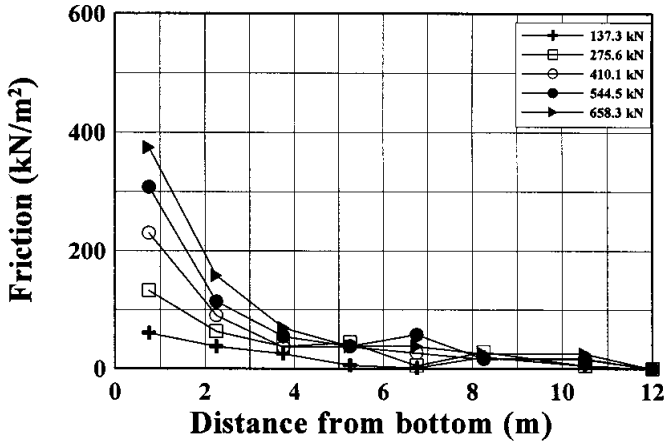

Figure 21. Grout-ground bond stress along the entire length of the ground anchor for compression-type anchor **(Kim, 2001)**.

6. LOAD TRANSFER THROUGH ADJACENT GROUND

The developed stresses inside the anchor surrounding soil are different according to the anchor type, whether it is tension-type or compression-type, and also according to the grouting stages, whether it is one-stage grouting or two-stage grouting. However, the two-stage grouted anchors have been abandoned since the '70s **(Barley and Windsor, 2000)**, so they are not considered herein.

According to the field and physical model tests of grouted anchors in the sand, the failure surface forms a cylinder close to the grouted body **(Hobst and Zajíc, 1983; Su and Fragaszy, 1988)**. The exact location of the failure cylinder depends on the relative strength of the interface between the grout and the adjacent soil **(Hanna, 1982)**.

(Hobst and Zajíc, 1983) presented and discussed the grouted anchor physical model test data. The model represents one-stage grouting, tension-type grouted anchor embedded in sand vertically and inclined from the horizon with an angle of 60^{o}. These tests were accomplished in the "Mining Institute Laboratory" by **(Kohoutek and Philip)**. **Figs. 21 and 22** present the stress distribution inside the surrounding soil for the vertical and inclined anchors, respectively.

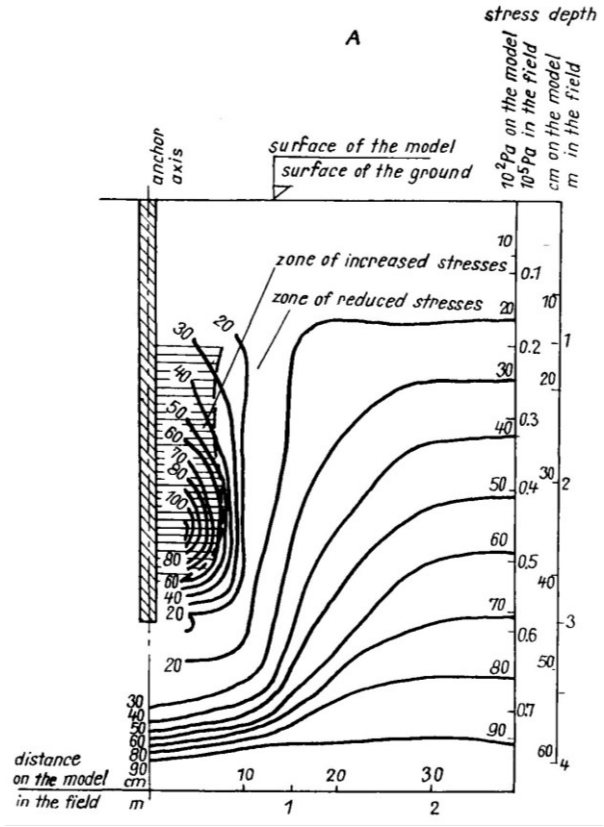

Figure 21. Stress distribution in the adjacent soil of the vertical anchor model **(Hobst and Zajíc, 1983)**.

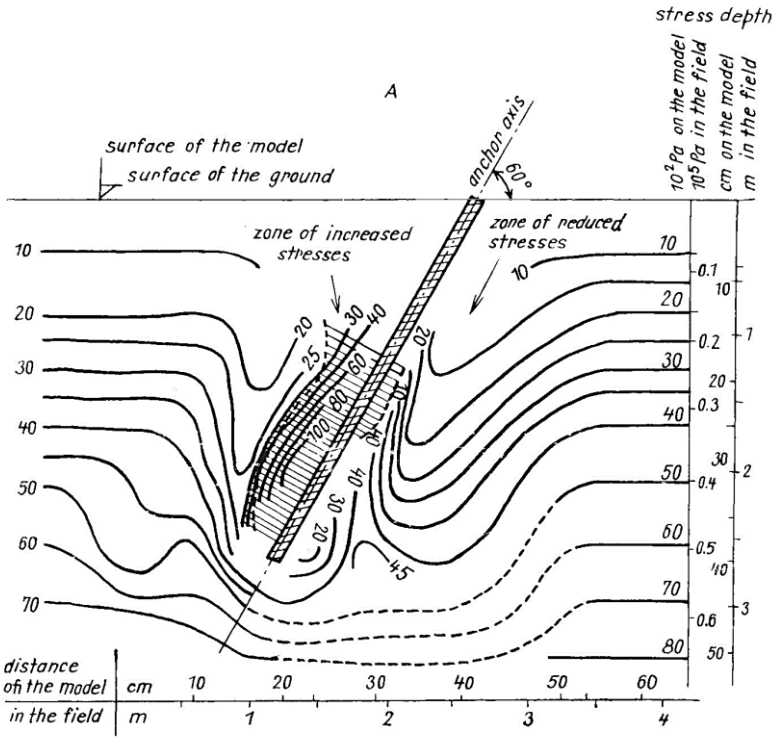

Figure 22. Stress distribution in the adjacent soil of the inclined anchor model **(Hobst and Zajíc, 1983)**

Both cases show that the surrounding soil, along the upper half of the bond length, after the shear strength of the grout-ground interface is exceeded, is subjected to compression stresses much more than the overburden stress. A relaxation of compression stress is noticed in the soil surrounding and below the lower half of the bond length. The effect of stress change is extended to (1m) away from the bond length in the case of the vertical anchor model, while the stress change zone is extended to almost twice as the case of the vertical anchor, i.e. (2m). It is also noticed that, in the case of an inclined anchor, the affected stress zone is larger on the side facing the ground surface. The inclined anchor model shows a greater pullout resistance than the vertical anchor due to the largely affected surrounding soil.

According to the same previous model tests, **(Hobst and Zajíc, 1983)** also stated that the pullout capacity is reduced by 50% or more when the bond length is embedded in a fully saturated sand layer instead of a dray sand layer. Improving the adjacent ground could improve the capacity of the anchor by increasing the grout-ground bond stress and the ground capacity **(Manassero, 2017)**.

7. ULTIMATE PULLOUT CAPACITY ESTIMATION

7.1 Semi-Empirical Methods:

In all the estimation methods of the ultimate capacity, only the grout-ground interface failure mode is considered because it is the most common failure mode in grouted ground anchors **(Barkhordari, 1998)**.

One of the earliest formulas used to estimate the ultimate capacity is suggested by **(Bauer, 1960) (as cited in Littlejohn, 1980)**. Eq. 3 is used for anchors with 150mm diameters embedded in granular soil. This Equation was adopted by **(BS 8081, 1989)**.

$$T_u = L\, n\, \tan \emptyset \tag{3}$$

where

(L) is the anchor bond length, (φ) is the angle of friction of the soil strata surrounding the anchor fixed length, (n) is an empirical factor depending on the drilling method, overburden pressure, and grouting pressure. The range of (n) values is 30-1000kN/m, a very wide range that could not be used without previous field tests. **(Littlejohn, 1970)**, depending on field tests suggested a more specific range 400-600kN/m for coarse sand and 130-165kN/m for fine sand.

(Littlejohn, 1970) suggested a more detailed Equation. Eq. 4 estimates the ultimate capacity, considering the anchor diameter, confining pressure, and overburden stress as individual factors. The end bearing of the proximal end of fixed length has also been considered.

$$T_u = A\, \acute{\sigma_v}\, \tan \emptyset\, \pi\, D\, L + B\, \gamma\, h\, (\pi/4)(D^2 - d^2) \tag{4}$$

Grout-ground bond stress+ End Bearing

where

(A) is the ratio between the confined pressure at the middle of the fixed length to the adjacent overburden pressure, which ranges between (1 and 2). The (A) value could be reduced to the (K_o, Coefficient of earth pressure at rest) value in the case of displaced soil

due to the installation of the casing, and there is no residual grouting pressure (the case of tremie grouting is included) **(Littlejohn, 1980)**.
(σ_v/) is the average effective overburden stress at the middle of the fixed length.
(d) is the diameter of the grouted body above the fixed length
(D) is the borehole diameter of the fixed length, which is equal to (3-4) d due to the permeability and compaction of the sand and the gravel.
(γ) is the effective soil density of the burden.
(h) is the depth of the proximal end of the fixed length
(B) is the bearing capacity factor
The second term of Eq. 4 is abandoned because the end bearing does not mobilize simultaneously with grout-ground bond stress (the first term), and it requires more displacement to mobilize **(Littlejohn, 1980)**. In addition, the second term deals with the enlargement of the fixed length due to the grouting pressure, which is out of the scope of the present research work. Both Eqs. 3 and 4 depend on the assumption of the uniform bond stress between the grout and the soil along the fixed length of the anchor, which is unrealistic and gives an overestimation value of the ultimate anchor capacity.
A rough estimation of anchor capacity could be made by using one of the two charts presented by **(Ostermayer, 1975; Ostermayer and Scheele, 1977)**, shown in **Fig.s 17 and 18,** respectively **(Barley and Windsor, 2000)**. These charts depend on soil type (properties) and fixed length. The nonlinear relation between the ultimate anchor capacity and the fixed length is considered within these charts.
The first term of Eq. 4 could be written in general form, as shown in Eqs. (5) and (6) **(Barley and Windsor, 2000)**:

$$T_u = \tau_{ult} A = \tau_{ult}\, \pi d L \quad (5)$$
$$T_u \propto L \quad (6)$$

where
(τ_{ult}) is the ultimate bond stress between the grout and the ground (skin friction),
(A) is the surface area of the anchor fixed length.
A nonlinear factor of proportionality is suggested to Eq. 6 by several researchers to take into account the nonuniform distribution of bond stress and the process of progressive debonding:
(Casanovas, 1989) introduced the apparent fixed anchor length representing the bond length at which the ultimate grout-ground bond stress could be mobilized. The apparent fixed length, as shown in Eq. 7, is used instead of the fixed length in Eq. 5.

$$L_{ve} = L^{\frac{1}{\log \tau_{ult}}} \quad (7)$$

where
(L_{ve}) is the apparent fixed anchor length in (m), the unit of ultimate grout-ground bond stress is in (ton/m^2).
Casanovas suggested using the Standard Penetration Test (SPT) number to calculate the ultimate grout-ground bond stress such as shown:

$$\tau_{ult} = 1.1\ N\ \{fine\ sand\}$$
$$\tau_{ult} = 1.5\ N\ \{medium\ sand\} \quad (8)$$
$$\tau_{ult} = 1.9\ N\ \{sand\ and\ gravel\}$$

where
The units of (τ_{ult}) in Eq. 8 is (ton/m^2), (N) is the SPT number represents the soil properties.
The apparent fixed length, as noticed in Eq.s 7 and 8 are a function of the anchor fixed length. **(Barley, 1995)** suggested to evaluate the efficiency factor (f_{eff}) as a function of the anchor bond length and the angle of internal friction of the surrounding soil such as:

$$f_{eff} = (0.91)^{L \tan \emptyset} \quad (9)$$

(Barkhordari, 1998) proposed a different efficiency factor, based on the back analysis of the field test data presented by **(Ostermayer, 1975; Ostermayer and Scheele, 1977)**. The proposed efficiency factor is also a function of anchor bond length and angle of friction, as shown in Eq. 10:

$$f_{eff} = \exp(-0.05\ L\ \tan \emptyset) \quad (10)$$

the efficiency factor calculated from Eq.s. 9 or 10 is introduced into Eq. 5 to produce Eq. 11 of estimation of the ultimate anchor capacity:

$$T_u = f_{eff}\ \tau_{ult}\ \pi d L \quad (11)$$

7.2 Field Test Methods

The field test is the most reliable method of estimating the ultimate anchor capacity, and the results indicate the behavior of the grouted ground anchor **(Littlejohn and Mothersille, 2008; Ruggeri et al., 2013)**. It is used to examine all the possible failure modes mentioned previously. This is done by testing anchor models until failure occurs with the same properties of working anchors embedded in the same soil in which the working anchors are embedded. All the most used codes **(BS 8081, 1989; DIN 4125, 1990; PTI, 2014)** recommend the field test with different methods and under different names. **(PTI, 2014)** suggests performing the "Preproduction test" for nonworking anchors during the design phase to find the ultimate grout ground bond stress since the maximum test load is (80%) of the specified minimum strength of the tendon. In addition, (PTI 2014) recommends performing two other types of tests for each of the working anchors. These tests are the Performance test and the Proof test. The performance test is performed for selected anchors not less than 5% of the total number of working anchors. The proof test is performed for the rest of the working anchors during the process of locking off (stressing the strand tendon with the design load and locking the anchor head) to examine the suitability of the anchor to the design load and the state of the apparent free length. The proof test load reaches (120% and 133%) of the design load for the temporary and permanent anchors, respectively.
Many researchers presented well-documented preproduction, performance, and proof tests for tension and compression anchors with various soil conditions **(Jacquard, 2014; Mothersille et al., 2015; Shapiro et al., 2017)**.

7.3 Numerical Methods

The numerical methods are the most feasible and reliable than the semi-empirical methods to obtain the ultimate anchor capacity and study the anchor behavior with different parameters. The accuracy of numerical methods' results depends on the accuracy of the used material properties, including the properties of the surrounding soil, and the suitability of the selected mathematical model. Many researchers have used different numerical and finite element methods to simulate the grouted ground anchor embedded into the soil, as shown below:
(Desai et al., 1986) modeled the grouted ground anchor with a 3-dimensional finite element using a FORTRAN written code. **(Kim, 2003; Bryson and Giraldo, 2020)** modeled the ground anchor using the Beam-Spring method, suggested by **(Coyle and Reese, 1966)**. **(Kim et al, 2006; Seo et al., 2019; Fabris et al., 2021)** have simulated the ground anchor with a 2-dimensional axisymmetric finite element model using well-known commercial software PLAXIS and ABAQUS. One-dimensional finite element has been used by **(Seo and Pelecanos, 2017; Smet et al., 2019; Al-Baghdadi et al., 2022)** for simplicity, timesaving, and feasibility. The output data from the site investigation reports could be used directly in one-dimensional modeling without complicated constitutive model parameters, which are needed in two- and three-dimensional modeling.

8. CONCLUSIONS

According to the conducted literature survey within the present study, the following conclusions could be outlined:

1) The bond stress along the tendon-grout and the grout-ground interfaces are not uniformly distributed along the tendon bond length and anchor bond length.
2) The confining pressure of the borehole on the grouted body significantly affects the grout strength, tendon-grout bond stress, and grout-ground skin friction.
3) Tendon nodes in the tendon bond length provide very high bond strength between the tendon and the grout.
4) All the available methods of estimating the ultimate pullout capacity of the anchor depend mainly on the grout-ground interface failure mode and do not consider the rest of the failure modes.
5) The anchor's ultimate capacity is not linearly proportioned with the tendon bond length. The feasible tendon bond length equals 6-7m. The anchor diameter has a small effect on the ultimate anchor capacity.
6) Adopting uniformly distributed grout-ground bond stress leads to overestimating the anchor's ultimate capacity.
7) In dense sand, the normal stress on the grout-ground interface exceeds the overburden stress by 2-10 times.
8) The inclined anchor has more capacity than the vertical anchor with the same average overburden pressure at the middle of the anchor bond length.
9) Improving the grout's tension properties by using cement additives, reinforcement, or both may enhance the bond strength of the tendon-grout interface and increase its ultimate capacity.

NOMENCLATURE

Symbol	Description	Symbol	Description
A	area, m^2.	N	Standard penetration test number.
d	Anchor diameter, mm.	n	Nondimensional factor.
E, E_m	modulus of elasticity, Mpa	r	Radius of the borehole, mm.
f_{eff}	Efficiency factor.	δ	displacement, mm.
K	Stiffness, kN/m.	υ, $υ_m$	Poisson's ratio.
L	Anchor bond length, m	τ	Skin friction, kPa.
L_a	apparent free length, m.	$τ_{ult}$	Ultimate skin friction, kPa.
L_{ve}	Apparent fixed length, m.	Ø	Angle of internal friction, degree.
T	ultimate load capacity, kN.		

Credit Authorship Contribution Statement

Nadher H. Al-Baghdadi: Writing – review & editing, Writing – original draft. Balqees A. Ahmed: Writing – review & editing.

Declaration of Competing Interest

The authors declare that they have no known competing financial interests or personal relationships that could have appeared to influence the work reported in this paper.

REFERENCES

Adams, D. A., and Littlejohn, G. S., 1997. Anchorage Load Transfer Studies using an Instrumented Full-scale Re-usable Laboratory Apparatus. In *Ground anchorages and anchored structures: Proceedings of the international conference organized by the Institution of Civil Engineers and held in London, UK, on 20–21 March*, pp. 411-421.

Al-Baghdadi, N.H., and Ahmed, B.A., 2022. Field tests of grouted ground anchors in the sandy soil of Najaf, Iraq. *Open Engineering*, 12(1), pp. 905-917. https://doi.org/10.1515/eng-2022-0359

Al-Baghdadi, N.H., Ahmed, B.A., and Al-Jorany, A.N., 2022. One-dimension finite element modeling of grouted ground anchor. *Engineering, Technology & Applied Science Research*, *12*(6), pp. 9752-9759. https://doi.org/10.48084/etasr.5325.

ASTM Standard C109/C 109M, 2002. Compressive strength of hydraulic cement mortars (Using 2-in. or [50-mm] Cube Specimens). ASTM International, West Conshohocken, PA, 19428-2959, United States.

Awad-Allah, M.F., 2018. Full-scale tests of ground anchors in alluvium soils of Egypt. *Lowland Technology International*, 20(1, June), pp. 15-26.

Barkhordari, K., 1998. The Influence of Load Transfer Mechanisms on Ground Anchor Design. Ph.D. Dissertation, University of Surrey, England, UK.

Barley, A D, 1978. A study and investigation of underreamed anchors and associated load transfer mechanism. Thesis, Marischal College, Aberdeen.

Barley, A.D., and Windsor, C.R., 2000. Recent advances in ground-anchor and reinforcement technology with reference to the development of the art. *International conference on geotechnics and geotechnical engineering, vol. 1, Melbourne, Australia. Basel, Lancaster,* pp. 1157-1252.

Barley, A.D., 1988. Ten Thousand Anchorages in Rock (Part I). *Ground Engineering*, September, 21(6), pp. 20-29.

Barley, A.D., 1995. Anchors in Theory and Practice. International Symposium on Anchors in Theory and Practice, Saltzburg, October.

Barley, A.D., 1996. Development of removable anchor systems and components. Keller Concrete Report - Confidential.

Barley, A.D., 1997. Properties of anchor grouts in a confined state. *In Ground anchorages and anchored structures: Proceedings of the international conference organized by the Institution of Civil Engineers and held in London, UK, on 20–21 March 1997* (pp. 13-22). Thomas Telford Publishing. https://doi.org/10.1680/gaaas.26070.0002b

Bauer, K, 1960. Injection of tie rods into unruly soil. Bau und Bauindustrie 14, pp. 520-522. (In Germany)

Benmokrane, B., Chekired, M., and Xu, H., 1995. Monitoring behavior of grouted anchors using vibrating-wire gauges. *Journal of geotechnical engineering*, 121(6), pp. 466-475. https://doi.org/10.1061/(ASCE)0733-9410(1995)121:6(466)

Briaud, J.L., III, W.F.P., and Weatherby, D.E., 1998. Should grouted anchors have short tendon bond length?. *Journal of geotechnical and geoenvironmental engineering*, 124(2), pp. 110-119. https://doi.org/10.1061/(ASCE)1090-0241(1998)124:2(110)

Brown, D.G., 1970. Uplift capacity of grouted rock anchors. Ontario hydro research quarterly, 22(4), pp. 18-24.

Bryson, L.S., and Giraldo, J.R., 2020. Analysis of case study presenting ground anchor load-transfer response in shale stratum. *Canadian Geotechnical Journal*, *57*(1), pp. 85-99. https://doi.org/10.1139/cgj-2018-0326

BS 8081, 1989, Code of practice for ground anchorages, British Standards Institution.

Bustamante, M., and Doix, B., 1985. Une methode pour Ie calcul des tirants et des micropieux injectes. Bulletin de liaison des Laboratoires des Ponts et Chaussees, No. 140, (As cited in Juran and Elias, 1991).

Casanovas, 1989. Bond Strength and Bearing Capacity of Injected Anchors: A New Approach. Proceedings of the 12th Conference SMFE, Rio De Janeiro, 1989 Volume 2.

Chalmovský, J., and Miča, L., 2018. The load-displacement behaviour of ground anchors in fine grained soils. Acta Polytechnica CTU Proceedings 16, pp. 18–24.

Chamberlain T. D., 1993. Investigation of expansive cements and their influence on the capacity of socketed piles and grouted anchors in rock. MEngSc (Research) Dissertation, Department of Civil Engineering, Monash University,

Coulter, S., and Martin, C.D., 2006. Effect of jet-grouting on surface settlements above the Aeschertunnel, Switzerland. *Tunnelling and underground space technology*, *21*(5), pp. 542-553. https://doi.org/10.1016/j.tust.2005.07.005

Coyle, H.M., and Reese, L.C., 1966. Load transfer for axially loaded piles in clay. Journal of the soil mechanics and foundations division, 92(2), pp. 1-26. https://doi.org/10.1061/JSFEAQ.0000850

Desai, C.S., Muqtadir, A., and Scheele, F., 1986. Interaction analysis of anchor-soil systems. Journal of geotechnical engineering, 112(5), pp. 537-553. https://doi.org/10.1061/(ASCE)0733-9410(1986)112:5(537)

DIN 4125, 1990, Ground Anchorages. Deutsches Institut für Normung, Berlin, Germany.

Elias, N., 2019. Development of innovative anchorage system for CFRP ground anchors (Doctoral dissertation, Swinburne University of Technology).

Evangelista, A., and Sapio, G., 1978. Behaviour of ground anchors in stiff clays. Proceedings of the 9th International Conference on Soil Mechanics and Foundation Engineering, Tokyo, Specialty Session 4, pp. 1-9. https://doi.org/10.1051/geotech/1978003039

Fabris, C., Schweiger, H.F., Pulko, B., Woschitz, H., and Račanský, V., 2021. Numerical simulation of a ground anchor pullout test monitored with fiber optic sensors. *Journal of Geotechnical and Geoenvironmental Engineering*, 147(2), P. 04020163. https://doi.org/10.1061/(ASCE)GT.1943-5606.0002442

FHWA, 1999. *Ground Anchors and Anchored Systems*. Federal Highway Administration, Washington D.C., USA.

Fujita, K., Ueda, K., and Kusabuka, M., 1977. A method to predict the load-displacement relationship of ground anchors. Specialty Session 4, Proceedings of the 9th International Conference on Soil Mechanics and Foundation Engineering, Tokyo, pp. 58-62.

Gilkey, H.J., Chamberlin, S.J., and Beal, R.W., 1940. Bond between Concrete and Steel reproduced in Eng. Report No. 26, Iowa Eng. Exp. Station, Iowa State Coll. pp. 25-147.

Hanna, T.H., 1982. *Foundation in tension, ground anchors*. Co-published by Trans Tech Publications, Germany, and McGraw-Hill Books Company, USA.

Hobst, L., and Zajíc, J., 1983. *Anchoring in Rock and Soil*. 2nd ed., Elsevier Scientific Publishing Company, Inc., Czechoslovakia.

Hyett, A. J., Bawden, W. F., and Reichert, R. D., 1992. The effect of rock mass confinement on the bond strength of fully grouted cable bolts. *Int. J. Rock Mech. Min. Sci. & Geomech. Abstr*., 29(5), pp. 503-524. https://doi.org/10.1016/0148-9062(92)92634-O

Hyett, A. J., Bawden, W. F., Macsporran, G. R., and Moosavi, M., 1995. A constitutive law for bond failure of fully-grouted cable bolts using a modified hoek cell. *International Journal Rock Mechanics & Mining Sciences*, 32(1), pp. 11-36. https://doi.org/10.1016/0148-9062(94)00018-X

Iten, M., and Puzrin, A. M., 2010. Monitoring of stress distribution along a ground anchor using BOTDA. *Sensors and Smart Structures Technologies for Civil, Mechanical, and Aerospace Systems*, 7647, pp. 779-793. https://doi.org/10.1117/12.847499

Jacquard, C., 2014. *Foundations by prestressing anchors of the Villa Méditerranée n Marseille: from design to monitoring*. In Soil-Structure Interaction, Underground Structures and Retaining Walls (pp. 127-131). IOS Press. https://doi:10.3233/978-1-61499-464-0-127

Jarred, D.J., and Haberfield, C.M., 1997. Tendon/grout interface performance in grouted anchors. Ground anchorages and anchored structures: Proceedings of the international conference

organized by the Institution of Civil Engineers and held in London, UK, on 20–21 March, pp. 3-12. https://doi.org/10.1680/gaaas.26070.0001

Juran, I., Elias, V., 1991. *Ground Anchors and Soil Nails in Retaining Structures*. In: Fang, HY. (eds) Foundation Engineering Handbook, Springer, Boston, MA.

Kaiser, P.K., Yazici, S., and Nose, J., 1992. Effect of stress change on the bond strength of fully grouted cables. *International Journal of Rock Mechanics and Mining Sciences & Geomechanics Abstracts*, 29(3), pp. 293-306. https://doi.org/10.1016/0148-9062(92)93662-4

Kim, N.K., 2001. Load transfer of tension and compression anchors in weathered soil. *Journal of the Korean Geotechnical Society*, 17(3), pp. 59-68.

Kim, N.K., 2003. Performance of tension and compression anchors in weathered soil. *Journal of Geotechnical and Geoenvironmental Engineering*, 129(12), pp. 1138-1150. https://doi.org/10.1061/(ASCE)1090-0241(2003)129:12(1138)

Kim, N.K., Park, J.S., and Kim, S.K., 2006. Numerical simulation of ground anchors. *Computers and Geotechnics*, 34(6), pp. 498-507. https://doi.org/10.1016/j.compgeo.2006.09.002

Klemenc, I., and Logar, J., 2013. In-situ Test of Permanent Prestressed Ground Anchors With Alternative Design Of Anchor Bond Length. Proceedings of the 18th International Conference on Soil Mechanics and Geotechnical Engineering, Paris, France.

Laldji, S., and Young, A.G., 1988. Bond between steel strand and cement grout in ground anchorages. Magazine of Concrete Research, 40(143), pp. 90-98. https://doi.org/10.1680/macr.1988.40.143.90

Littlejohn, G.S., 1970. Soil anchors. ICE conf on Ground Engineering, London

Littlejohn, G.S., and Bruce, D.A., 1975. Rock anchors-state of the art. Part 1: design. Ground Engineering, 8(3), pp. 25 – 32.

Littlejohn, G.S., 1979, October. Ground anchors: state-of-the-art. In Symp on Prestressed Ground Anchors Conc Soc of SA.

Littlejohn, G.S., 1980. Design estimation of the ultimate load-holding capacity of ground anchors. *Ground Engineering*, 13(8), pp. 25-39.

Littlejohn, G.S., and Bruce, D.A., 1975. Rock Anchors State of Art- Part 1: Design. *Ground Engineering*, 8(3), pp. 25 – 32.

Littlejohn, G.S., Bruce, D.A., and Deppner, W., 1977. Anchor Field Tests in Carboniferous Strata. *9th International Conference on Soil Mechanics and Foundation Engineering, Tokyo, Japan*, Speciality Session 4, pp. 82-86.

Littlejohn, S., and Mothersille, D., 2008. Maintenance and monitoring of anchorages: guidelines. *Proceedings of the Institution of Civil Engineers-Geotechnical Engineering*, 161(2), pp. 93-106. https://doi.org/10.1680/geng.2008.161.2.107

Lo, Yuen-Cheong, 1979. Investigation of the effect of lateral restraint on ground anchor failure at the grout/tendon interface. Thesis, University of Sheffield, Civil Engineering.

Manassero, V., 2017. An Unconventional Application of Jet Grouting to Install 4900 kN Ground Anchors in Loose Alluvial Soil. *In Grouting*, ASCE, (pp. 31-41). https://doi.org/10.1061/9780784480809.004

Mastrantuono, C., and Tomiolo, A., 1977. First application of a totally protected anchorage. *Proceedings of the 9th International Conference on Soil Mechanics and Foundation Engineering, Specialty Session, Tokyo*, pp. 107–112.

Ortigao, J.A.R., 1996, November. FRP applications in geotechnical engineering. In *Proc. ASCE 4th Materials Engineering Conference, Washington DC* (Vol. 1, pp. 535-544).

Mothersille, D., Duzceer, R., Gokalp, A., and Okumusoglu, B., 2015. Support of 25 m deep excavation using ground anchors in Russia. *Proceedings of the Institution of Civil Engineers-Geotechnical Engineering,* 168(4), pp. 281-295. https://doi.org/10.1680/geng.14.00043

Ostermayer H., 1975. Construction carrying behavior and creep characteristics of ground anchors. *Int. Conf. On Diaphragm Walls and Anchorages*. I.C.E. London, 18-20, pp. 141-151.

Ostermayer, H., and Scheele, F., 1977. Research on ground anchors in non-cohesive soils. *Proceedings of the 9th International Conference on Soil Mechanics and Foundation Engineering, Tokyo, Japan*, Specialty Session 4, pp. 92-97.

Popa, H., Ene, A., and Marcu, D., 2016. Instrumentation and measurements of a ground anchor for a retaining structure. *EUROFUGE 2016 3rd European Conference on Physical Modelling in Geotechnics.*

PTI, 2014. Recommendations for Prestressed Rock and Soil Anchors. 5th ed. Post Tensioning Institute, Phoenix, Arizona, USA.

Ruggeri, P., Segato, D., and Scarpelli, G., 2013. Sheet pile quay wall safety: investigation of posttensioned anchor failures. Journal of Geotechnical and Geoenvironmental Engineering, 139(9), pp. 1567-1574. https://doi.org/10.1061/(ASCE)GT.1943-5606.0000886

Ruggeri, P., Fruzzetti, V.M., and Scarpelli, G., 2020. The Behavior of a Thread-Bar Grouted Anchor in Soils from Local Strain Monitoring. *Applied Sciences*, 10(20), p.7194. https://doi.org/10.3390/app10207194

Seo, H., and Pelecanos, L., 2017, December. Load transfer in soil anchors–Finite Element analysis of pull-out tests. *In 8th International Conference on Structural Engineering and Construction Management*.

Seo, H.J., Marketos, G., and Pelecanos, L., 2019. Soil-structure interaction in field pull-out tests of soil anchors and additional resistance from the reaction plate. *In XVII Europian Conference on Soil Mechanics and Geotechnical Engineering, Reykjavik, Iceland* (pp. 1-8). https://doi:10.32075/17ECSMGE-2019-0390

Shapiro, S., Cennamo, A., and Stanbury, J., 2017. Settlement Control Meets Flood Control—Hybrid Compaction Grouted Ground Anchors for NYU Langone Medical Center's Kimmel Pavilion. *In Grouting*, ASCE, (pp. 250-259). https://doi.org/10.1061/9780784480793.024

Shokri, B.J., Entezam, Sh., Nourizadeh, H., Motallebiyan, A., Mirzaghoranali, A., McDougall, K., Aziz, N., and Karunasena, K., 2023. The Effect of changing confinement diameter on axial load transfer mechanisms of fully grouted rock bolts. *Proceedings of the 2023 Resource Operators Conference,* pp. 290-295.

Smet, J., Huybrechts, N., Lysebetten, G.V., Verstraelen, J., and François, S., 2019. Optical fiber strain measurements and numerical modeling of load tests on grouted anchors. *Journal of Geotechnical and Geoenvironmental Engineering*, 145(12), p.04019103. https://doi.org/10.1061/(ASCE)GT.1943-5606.0002167

Sousa, A.M.D.D., Costa, Y.D.J., Florêncio, L.A.D.S., and Costa, C.M.L., 2021. Load transfer on instrumented prestressed ground anchors in sandy soil. *Revista IBRACON de structures materials*, 14, e14612. https://doi.org/10.1590/S1983-41952021000600012

Stocker, M.F., and Sozen, M.A., 1969. Investigation of prestressed reinforced concrete for highway bridges, part vi, bond characteristics of prestressing strand. Civil Engineering Studies SRS-344.

Su, W., and Fragaszy, R.J., 1988. Uplift testing of model anchors. *Journal of Geotechnical Engineering Division*, 114 (9), pp. 961-983. https://doi.org/10.1061/(ASCE)0733-9410(1988)114:9(961)

Weerasinghe, R.B., and Littlejohn, G.S., 1997. Load transfer and failure of anchorages in weak mudstone. In Ground anchorages and anchored structures: Proceedings of the international conference organized by the Institution of Civil Engineers and held in London, UK, on 20–21 March 1997 (pp. 34-44). Thomas Telford Publishing. https://doi.org/10.1680/gaaas.26070.0004

Wernick, R., 1977. Stresses and strains on the surfaces of anchors. Specialty Session 4, Proceedings of the 9th International Conference on Soil Mechanics and Foundation Engineering, Tokyo, pp. 113-119.

Zhang, B., Benmokrane, B., Chennouf, A., Mukhopadhyaya, P., and El-Safty, A., 2001. Tensile behavior of FRP tendons for prestressed ground anchors. *Journal of Composites for Construction*, 5(2), pp. 85-93. https://doi.org/10.1061/(ASCE)1090-0268(2001)5:2(85)

قابلية التحمل القصوى و آلية نقل الحمل للمرساة الأرضية المطمورة في الترب الحبيبية: مراجعة تاريخية

ناظر حسن البغدادي[1,*] , بلقيس عبد الواحد أحمد[2]

[1] قسم الهندسة المدنية, كلية الهندسة, جامعة الكوفة, النجف, العراق
[2] قسم الهندسة المدنية, كلية الهندسة, جامعة بغداد, بغداد, العراق

الخلاصة

إن المرساة الأرضيّة المحشيّة بالملاط الاسمنتي هي من العناصر الجيوتقنية الأكثر استخدامًا لنقل حمل الشد من البنية الفوقية أو كتلة التربة الأمامية لسطح الفشل المحتمل (المنطقة الفعالة) إلى طبقة تربة أعمق وأكثر كفاءة, من أجل موثوقيتها وجدواها. يتم اِنشاؤه بشكل عام عن طريق إدخال وتر، عادةً مصنوعة من الفولاذ المجدول مسبق الجهد، في بئر مملوءة بالملاط الإسمنتي. تم استخدامه بنجاح في سد شيورفاس في الجزائر في عام (1934). ووفقًا لآلية نقل الحمل، هناك نوعان من المراسِ الأرضيّة؛ نوع الشد ونوع الضغط. تشير أسماء هذين النوعين من المراسِ إلى الاِجهادات المتكونة في جسم المرساة الاسمنتي. تم استعراض العديد من العوامل التي تؤثر على آلية نقل الحمل. والعامل الرئيسي الذي يؤثر على آلية نقل الحمل هو الضغط الحاصر المحيطي المؤثر على جسم المرساة الاسمنتي. يقدم البحث الحالي مسحًا أدبيًا للدراسات التي تتناول آلية نقل الحمل لكلا النوعين من المرساة الارضية: نوع الشد ونوع الضغط والمطمورة في التربة الحبيبية. وكذلك تمت مراجعة ومناقشة الطرق التي تم تطويرها مؤخرًا لتقدير قابلية السحب القصوى للمرساة.

الكلمات المفتاحية: المرساة الأرضية, ألية نقل الحمل, قابلية السحب القصوى.